DOCUMENT CONTROL SHEET

	ORIGINATOR'S REF.		SECURITY CLASS.
	NLR TP 96117 U		Unclassified

ORIGINATOR
National Aerospace Laboratory NLR, Amsterdam, The Netherlands

TITLE
Theory of sound propagation in a flow duct lined with annular segments of porous material

PRESENTED AT

AUTHORS	DATE	pp	ref
P. Sijtsma	960215	35	12

DESCRIPTORS

Acoustic ducts	Propagation modes
Engine values	Sound transmission
Engine inlets	
Linings	
Noise reduction	
Porous materials	

ABSTRACT
A theory is presented to calculate acoustic modes in a circular flow duct lined with porous material. The porous material is divided into annular segments by a rigid structure, which prevents axial sound propagation from one segment into the other. Single modes cannot exist in such a configuration, but it is shown that approximate solutions of the eigenvalue problem can be constructed. A numerical example is given and compared with special cases from the literature.

NLR TECHNICAL PUBLICATION

TP 96117 U

THEORY OF SOUND PROPAGATION IN A FLOW DUCT LINED WITH ANNULAR SEGMENTS OF POROUS MATERIAL

by

P. Sijtsma

This investigation has been carried out under a contract awarded by the Netherlands Agency for Aerospace Programs, contract number 01309N.

Division : Fluid Dynamics
Prepared : PS/
Approved : HHB/

Completed : 960215
Order number : 101.315
Typ. : JS

Summary

A theory is presented to calculate acoustic modes in a circular flow duct lined with porous material. The porous material is divided into annular segments by a rigid structure, which prevents axial sound propagation from one segment into the other. Single modes can not exist in such a configuration, but it is shown that approximate solutions of the eigenvalue problem can be constructed. A numerical example is given and compared with special cases from the literature.

Contents

(35 pages in total)

Symbols

A	constant introduced in (6)
B_k	constants introduced in (9), given by (31)
b	duct radius including liner thickness, $b = 1+d$
c_k	coefficients given by (22)
d	liner thickness, $d = b-1$
F_m	function defined by (18)
G_m	function defined by (19)
i	imaginary unit
J_m	m-th order Bessel function of the first kind
L	pitch length, $L = x_2-x_1$
M	axial flow Mach number
m	circumferential wave number
p	acoustic pressure
Q_k	constants defined by (30)
q_k	coefficients defined by (34)
r	radial coordinate
t	time
$\boldsymbol{u}$	acoustic velocity vector
u_n	acoustic velocity component normal to perforate plate
x	axial coordinate
x_1,x_2	axial coordinates of porous segment edges
Y_m	m-th order Bessel function of the second kind
Z_0	impedance of perforate plate
Z_c	characteristic impedance of porous material

Greek

α	axial wave number
ε	radial wave number, defined by (7)
θ	circumferential coordinate
λ	parameter $0 \leq \lambda \leq 1$, introduced in (27)
μ	propagation constant of porous material
μ_k	constants defined by (10)
ξ	parameter introduced in (20)
ω	frequency

Superscripts

$(..)^{-}$	in duct
$(..)^{+}$	in porous material

1 Introduction

Fan noise generated by an aircraft turbofan engine is usually attenuated by a so-called locally reacting liner, mounted in the inlet duct wall. Such a liner consists of a honeycomb array of air-filled cavities, covered with a perforate plate.

The characteristics of a locally reacting liner can be chosen to maximize the attenuation of a sound field of single frequency and single (circumferential and radial) mode. This is achieved by choosing the liner cavity depth and the resistance of the perforate plate such that the optimum effective wall impedance (ratio between acoustic wall pressure and acoustic velocity normal to the wall) is realized for such a specific acoustic wave.

However, the sound field in an engine inlet consists of several frequencies, which depend on the flight condition. Furthermore, due to non-axisymmetry in geometry and inflow, scattering occurs from prevailing circumferential modes near the fan to other modes towards the inlet. For each circumferential mode, several radial modes may be present.

A locally reacting liner can provide maximum attenuation for one acoustic mode, but for the other modes the wall impedance is different from the optimum and the attenuation will be less than possible. Therefore, it is interesting to consider acoustic treatment for which the sound attenuation is less frequency and mode number sensitive than for a locally reacting liner.

A possible alternative is a bulk-absorbing liner consisting of a layer of some porous material in the inlet duct wall (Fig. 1). This porous material is covered with a perforate plate or sheet and it may, for structural reasons, be embedded in a rigid structure of annular partitions (Fig. 2). Bulk-absorbing liners or briefly 'bulk-absorbers' have a reputation to be less mode and frequency dependent than locally reacting liners (Refs. 1, 2, 3, 4).

An advantage of bulk-absorbers compared with locally reacting liners is the larger number of available degrees of freedom for liner optimization. Besides varying the liner thickness and the properties of the perforate plate, it is also possible to vary the acoustic properties of the porous material.

To calculate the noise reduction that can be obtained with bulk-absorbers, it is necessary to have a design procedure which is similar to the procedure followed for optimizing a locally reacting liner. In locally-reacting liner design, often a modal analysis (e.g. Ref. 5) is used, where the engine inlet is modelled by a duct of constant circular cross-section, with a uniform axial flow in it. The duct is then divided into three sections: two hard-wall sections and a lined section in

between (Fig. 3).

One of the key problems in a modal analysis is the determination of the eigenvalues and corresponding mode shapes in the lined section. Consequently, as soon as we have an algorithm to determine the eigenvalues in a section lined with a bulk-absorber, it can be readily incorporated in an existing liner design procedure and a fair comparison with locally reacting liners can be made.

A number of investigators (e.g. Refs. 4, 6, 7, 8) has studied the eigenvalue problem in a circular duct lined with a bulk-absorber. The eigenvalues were calculated under the assumption of an infinitely long layer of porous material. The first who stated the eigenvalue problem was Scott (Ref. 9).

In this paper, a theory is presented to calculate modes in a circular duct lined with porous material, which is divided into annular segments (Fig. 2). The annular partitions which separate the segments prevent sound propagation from one segment to the other. The partitions are modelled as hard fences of zero thickness, where reflections occur. It is assumed that each segment has the same axial length L (Fig. 2).

The porous material is assumed to be homogeneous and isotropic. Furthermore, it is assumed to be rigid, like glass fibre or metallic foam, so that the sound propagation is mainly through the pores and not through the material itself. As a result, we can use the theory as described in references 2, 3 and 10. The propagation of sound inside the porous material then is essentially described by two complex quantities, the characteristic impedance and the propagation constant, which are both frequency dependent.

Duct modes can be constructed by coupling the acoustic field inside the duct with the acoustic field inside the segments of porous material. Inside the duct, a single mode is prescribed with unknown axial wavenumber α and, using the boundary conditions at the interface, the sound field inside the porous material is calculated. Those α's (the "eigenvalues") are determined for which non-zero solutions exist.

Rienstra (Ref. 11) treated a limit case of this bulk-absorber eigenvalue problem, viz. the case where L is infinitesimally small (say $L \rightarrow 0$). The case of no annular partitioning (say $L \rightarrow \infty$) is covered by the theory of Scott (Ref. 9). In practical applications, however, the pitch length is probably such that neither of these two limit cases yields a good approximation.

In the present work, the "pitch" L may vary from very small to very large. A complication is, however, that no single-mode solutions of this eigenvalue problem exist. This is due to the reflections which occur at the partitions (Fig. 4). Nevertheless, approximate solutions can be constructed successfully.

In the following chapter, the problem will be formulated mathematically. Then, it is explained why single modes can not exist and how approximate eigenvalues can be found. Numerical examples are presented and compared with the limit cases $L \to 0$ and $L \to \infty$.

2 Formulation of the problem

In this paper, all physical quantities have been made dimensionless using the ambient speed of sound, the ambient air density and the duct inner radius. A hub is not included in this study. In the duct, cylindrical coordinates (x,r,θ) are defined. An acoustic field of single (non-dimensional) frequency ω will be considered and the factor $\exp(i\omega t)$ is suppressed throughout. The thickness of the perforate plate and the partition fences is neglected.

2.1 Governing equations

The acoustic pressure p inside the duct ($r \leq 1$) is governed by the convective Helmholtz equation

$$\nabla^2 p + \left(\omega - iM\frac{\partial}{\partial x} \right)^2 p = 0 , \tag{1}$$

where M is the Mach number of the uniform steady flow. The acoustic velocity $\boldsymbol{u}$ is related to the pressure via the momentum equation as follows:

$$i\left(\omega - iM \frac{\partial}{\partial x} \right)\boldsymbol{u} + \nabla p = 0 . \tag{2}$$

In the porous material ($1 \leq r \leq b$), where there is no steady flow, the Helmholtz equation and the momentum equation read:

$$\nabla^2 p + \mu^2 p = 0 , \tag{3}$$

$$i\mu Z_c \boldsymbol{u} + \nabla p = 0, \tag{4}$$

where μ is the so-called propagation constant and Z_c is the characteristic impedance (Refs. 2, 3, 10).

2.2 Mode shapes

A single mode inside the duct is described by

$$p^{-}(x,r,\theta) = f^{-}(r) e^{i(\alpha x + m\theta)}. \tag{5}$$

From the Helmholtz equation (1) it follows that we can write:

$$p^{-}(x,r,\theta) = A\, J_m(\varepsilon r)\, e^{i(\alpha x + m\theta)}, \tag{6}$$

where A is some constant, J_m is the m-th order Bessel function of the first kind and ε is given

by the dispersion relation:

$$\varepsilon^2 = (\omega + M\alpha)^2 - \alpha^2. \tag{7}$$

Inside a segment of porous material, bounded by the hard-wall fences at $x = x_1$ and $x = x_2$ (with $x_2 - x_1 = L$), we can write:

$$p^+(x,r,\theta) = \sum_{k=0}^{\infty} f_k^+(r) \cos\left(\frac{k\pi(x-x_1)}{L}\right) e^{im\theta}. \tag{8}$$

By applying the Helmholtz equation (3) and the hard-wall boundary condition at $r = b$ ($\partial p/\partial r = 0$), we find

$$p^+(x,r,\theta) = \sum_{k=0}^{\infty} B_k \left\{ J_m(\mu_k r) Y_m'(\mu_k b) - Y_m(\mu_k r) J_m'(\mu_k b) \right\} \cos\left(\frac{k\pi(x-x_1)}{L}\right) e^{im\theta}, \tag{9}$$

where B_k are constants and Y_m is the m-th order Bessel function of the second kind. The constants μ_k are given by

$$\mu_k^2 = \mu^2 - \left(\frac{k\pi}{L}\right)^2. \tag{10}$$

2.3 Boundary conditions

Across the perforate plate (at $r = 1$) the normal velocity has to be continuous, in other words:

$$u_n^- = u_n^+ . \tag{11}$$

To obtain an expression in terms of p^- and p^+, one can not directly apply (2) for the left hand side. The reason for this is that the steady flow is not continuous across the perforate plate. To obtain the correct expression for u_n^-, a precise analysis, as in references 5 and 12, has to be carried out with a boundary layer of vanishing thickness. The result is:

$$\frac{i\omega}{(\omega+M\alpha)^2}\frac{\partial p^-}{\partial r} = -\frac{1}{i\mu Z_c}\frac{\partial p^+}{\partial r} . \tag{12}$$

From (6) and (9) then follows:

$$\frac{i\omega}{(\omega+M\alpha)^2} A\ \varepsilon J_m'(\varepsilon) e^{i\alpha x} =$$

$$-\frac{1}{i\mu Z_c} \sum_{k=0}^{\infty} B_k \mu_k \left\{ J_m'(\mu_k) Y_m'(\mu_k b) - Y_m'(\mu_k) J_m'(\mu_k b) \right\} \cos\left(\frac{k\pi(x-x_1)}{L} \right). \tag{13}$$

The second boundary condition at $r = 1$ is the relation between the pressure jump across the perforate plate and the normal velocity through it:

$$p^- - p^+ = Z_0\ u_n\ , \tag{14}$$

where Z_0 is the impedance of the plate. With (6) and (9), it follows that

$$A J_m(\varepsilon) e^{i\alpha x} - \sum_{k=0}^{\infty} B_k \left\{ J_m(\mu_k) Y_m'(\mu_k b) - Y_m(\mu_k) J_m'(\mu_k b) \right\} \cos\left(\frac{k\pi(x-x_1)}{L} \right) = Z_0 u_n\ . \tag{15}$$

In the right hand side of (15), one can substitute for u_n either the left hand side or the right hand side of (13).

Redefining the constants A and B_k, we can write instead of (13) and (15):

$$\frac{i\omega}{(\omega+M\alpha)^2} A\ e^{i\alpha x} = -\frac{1}{i\mu Z_c} \sum_{k=0}^{\infty} B_k \cos\left(\frac{k\pi(x-x_1)}{L} \right), \tag{16}$$

$$A\ F_m(\varepsilon) e^{i\alpha x} - \sum_{k=0}^{\infty} B_k G_m(\mu_k, b) \cos\left(\frac{k\pi(x-x_1)}{L} \right) = Z_0 u_n\ , \tag{17}$$

where the auxiliary functions F_m and G_m are defined by

$$F_m(\varepsilon) = \frac{J_m(\varepsilon)}{\varepsilon J_m'(\varepsilon)}\ , \tag{18}$$

$$G_m(\mu_k, b) = \frac{J_m(\mu_k) Y_m'(\mu_k b) - Y_m(\mu_k) J_m'(\mu_k b)}{\mu_k \left\{ J_m'(\mu_k) Y_m'(\mu_k b) - Y_m'(\mu_k) J_m'(\mu_k b) \right\}}\ . \tag{19}$$

In Appendix A, the boundary conditions are described for the limit cases $L \to 0$ and $L \to \infty$. Also the relation with a locally reacting liner is shown there.

3 Solution

In this chapter, it will be shown that the boundary conditions for a single duct mode, (16) and (17), can not hold simultaneously. In other words, it will be shown that single modes can not exist. A method to calculate approximate solutions is presented.

3.1 The impossibility of an exact solution

In the right hand side of (17), we can substitute for u_n either the left hand side or the right hand side of (16). The most general expression for u_n is a linear combination of both:

$$u_n = \xi \frac{i\omega}{(\omega+M\alpha)^2} A e^{i\alpha x} + (1-\xi)\frac{-1}{i\mu Z_c}\sum_{k=0}^{\infty} B_k \cos\left(\frac{k\pi(x-x_1)}{L}\right), \tag{20}$$

for some real number ξ. For convenience, we write:

$$e^{i\alpha x} = \sum_{k=0}^{\infty} c_k(\alpha) \cos\left(\frac{k\pi(x-x_1)}{L}\right), \tag{21}$$

with

$$c_k(\alpha) = \begin{cases} \dfrac{e^{i\alpha x_2} - e^{i\alpha x_1}}{i\alpha L}, & \text{for } k=0, \\ \dfrac{2\left(e^{i\alpha x_2}(-1)^k - e^{i\alpha x_1}\right)}{i\alpha L\left(1 - (k\pi)^2/(\alpha L)^2\right)}, & \text{for } k>0. \end{cases} \tag{22}$$

Herewith, (16) and (17) are transformed into:

$$\sum_{k=0}^{\infty} \cos\left(\frac{k\pi(x-x_1)}{L}\right)\left\{\frac{i\omega}{(\omega+M\alpha)^2}Ac_k(\alpha) - \frac{-1}{i\mu Z_c}B_k\right\} = 0, \tag{23}$$

$$\sum_{k=0}^{\infty} \cos\left(\frac{k\pi(x-x_1)}{L}\right)\left\{\left[F_m(\varepsilon) - \xi Z_0\frac{i\omega}{(\omega+M\alpha)^2}\right]Ac_k(\alpha) - \left[G_m(\mu_k,b) + (1-\xi)Z_0\frac{-1}{i\mu Z_c}\right]B_k\right\} = 0. \tag{24}$$

It is seen that we can <u>not</u> simultaneously satisfy (23) and (24), unless the constants A and B_k are zero. In other words, single modes like (5) can not exist in a duct lined with segments of porous material.

3.2 Approximation

To obtain an approximate solution we write equation (23) briefly as

$$\Delta u_n(x) = 0 \tag{25}$$

and (24) as

$$\Delta p(x) - Z_0 u_n(x) = 0. \tag{26}$$

We will minimize

$$\frac{1}{\lambda(\lambda-1)L}\int_{x_1}^{x_2}\left(\lambda|\Delta u_n(x)|^2 + (\lambda-1)|\Delta p(x) - Z_0 u_n(x)|^2\right)dx, \tag{27}$$

for some λ, with $0 \le \lambda \le 1$. If $\lambda = 0$, then the constants B_k follow immediately from (24), hence (26) is solved exactly, and (25) is minimized in the least squares sense as a function of α. Conversely, if $\lambda = 1$, then (25) is solved exactly and (26) is minimized as a function of α.

Optimizing for B_k with any λ, the minimum is

$$E_0(\alpha) + \frac{1}{2}\sum_{k=1}^{\infty} E_k(\alpha), \tag{28}$$

with

$$E_k(\alpha) = Q_k \left| \frac{i\omega}{(\omega+M\alpha)^2} c_k(\alpha) A \left(\frac{(\omega+M\alpha)^2}{i\omega} F_m(\varepsilon) - [Z_0 - i\mu Z_c G_m(\mu_k,b)] \right) \right|^2, \tag{29}$$

$$Q_k = \frac{1}{\lambda + (1-\lambda)\,|(1-\xi)Z_0 - i\mu Z_c G_m(\mu_k,b)\,|^2}, \tag{30}$$

found for

$$\begin{aligned} B_k = & - i\mu Z_c \frac{i\omega}{(\omega+M\alpha)^2} Q_k c_k(\alpha) A \\ & \times \left\{ \lambda + (1-\lambda) \left((1-\xi)Z_0 - i\mu Z_c G_m(\mu_k,b) \right)^* \left(\frac{(\omega+M\alpha)^2}{i\omega} F_m(\varepsilon) - \xi Z_0 \right) \right\}, \end{aligned} \tag{31}$$

where the asterisk denotes the complex conjugate.

The sought eigenvalues α are the locations of the minima of (28). They still depend on the choice for λ and ξ, which only occur in the constants Q_k. This dependency on λ and ξ is small, as will be illustrated in the next chapter. Moreover, a choice has to be made for x_1, x_2 and A. This can be done by giving $A\exp(i\alpha x)$ a fixed value halfway x_1 and x_2, which can be realized by choosing

$$x_1 = -\frac{L}{2}, \quad x_2 = \frac{L}{2}, \quad A = 1. \tag{32}$$

Fixing $A\exp(i\alpha x)$ for an other value of x comes down to adding a factor $\exp(i\alpha x_0)$ in (29).

3.3 Solution procedure

The minima of (28) can be localized in two steps.

First, minimize (28), as if $c_k(\alpha)/(\omega+M\alpha)^2$ were independent of α. Solutions of this "minimization" follow from:

$$\frac{(\omega+M\alpha)^2}{i\omega} F_m(\varepsilon) + i\mu Z_c \frac{\sum_{k=0}^{\infty} q_k(\alpha) G_m(\mu_k,b)}{\sum_{k=0}^{\infty} q_k(\alpha)} = Z_0, \tag{33}$$

where

$$q_k(\alpha) = \begin{cases} |Q_k c_k(\alpha)|^2, & \text{for } k=0, \\ \frac{1}{2}|Q_k c_k(\alpha)|^2, & \text{for } k>0. \end{cases} \tag{34}$$

Solutions of (33) can be found, for instance, with the Secant Method, using solutions of $F_m(\varepsilon) = 0$ and $F_m(\varepsilon) = \infty$ (hard wall) as start values.

Secondly, minimize (28) with some minimum search routine using the solutions of (33) as initial values. It appears that these initial guesses are close to the eventual solutions, especially when αL is not too large, say $|\alpha L| \leq 10$. This is illustrated in the next chapter.

If αL is very small, say $|\alpha L| \leq 0.2$, then $q_0(\alpha)$ is the dominant term and (33) degenerates into the limit case $L \rightarrow 0$, given by equation (A.7) in Appendix A.

4 Numerical example

4.1 Case definition

Consider a duct of radius 0.5 m and a sound field of 2150 Hz, which can be representative for an aircraft engine. If the speed of sound is 340 m/s, then the dimensionless frequency is

$$\omega = 19.866.$$

The following dimensionless parameters are assumed:

circumferential mode number	$m = 5,$
axial flow Mach number	$M = 0.3,$
impedance of perforate plate	$Z_0 = 1.5 + 0.1i,$
liner thickness	$d = 0.05.$

For the pitch L, a series of values is considered, namely:

$$L = 0.04\ ,\ 0.08\ ,\ 0.12\ ,\ 0.16\ ,\ 0.20,\ 0.28\ ,\ 0.40\ ,\ 0.60\ ,\ 1.00\ ,\ 2.00\ .$$

Moreover, the limit cases $L \to 0$ and $L \to \infty$ (see Appendix A) are considered.

The values of the acoustic properties of the porous material, Z_c and μ, are from recent measurements on the metallic foam "Retimet":

characteristic impedance	$Z_c = 1.3 - 0.23i,$
propagation constant	$\mu = 26 - 7.0i.$

Choices have to be made for the constants λ and ξ. First, λ has to be chosen such that (27) yields a good balance between (25) and (26). In this case we have chosen:

$$\lambda = 0.75.$$

The constant ξ can be chosen arbitrarily, however, it is seen from (30) that a small ξ results in a small value for (28). We chose for:

$$\xi = -1.0\ .$$

In the following, it is shown that the choices for λ and ξ are not very critical.

4.2 Results

In figure 5, solutions are plotted of minimizing (28) for the above range of L's. The limit cases $L \to 0$ and $L \to \infty$ are included. Two things are notable in this figure.

First, there are certain modes (two in the figure) which only occur for the limit case $L \to \infty$. These are modes for which the sound propagation is mainly through the layer of porous material. Such modes are not present as long as L is finite. The appearance of these special "bulk modes" makes it uncertain that results for larger and larger L tend to the limit case $L \to \infty$. However, if the imaginary part of μ is not too small, the energy transported in such modes is low and the limit case will be approximately the same as the limit for L increasing to infinity.

The second observation from figure 5 is that the choice of L seems to be irrelevant for the downstream modes (upper left part in the figure) and also for the upstream "cut-off" modes (solutions with a large absolute imaginary part). Only for the upstream "cut-on" modes (the rightmost solutions), the pitch length L seems to be relevant.

In figure 6, an enlargement is shown of figure 5 around these upstream "cut-on" modes. It is observed that the solutions for finite L vary between both limit cases along whimsical paths. The limiting behaviour towards the case $L \to \infty$ is indeed not fully convincing.

In figures 7 and 8 is shown how well the boundary conditions (16) and (17), respectively, are satisfied. This is done for the eigenvalue $\alpha = 21.66–2.03i$, which is a solution for $L = 0.20$.

4.3 Comparison with initial values

It is interesting to see how well the initial guesses, i.e., the solutions of (33), compare with the eventual solutions of (28). The result of this comparison is shown in figure 9. For small L, say $L < 0.5$, the solutions of (33) are good approximations of the solutions of (28). For larger L, some distance develops between the solutions of (28) and (33).

4.4 Influence of λ and ξ

An other interesting question is how strongly the eigenvalues depend on λ and ξ. In the results presented above we had $\lambda = 0.75$ and $\xi = -1$. If we keep ξ the same and choose $\lambda = 0$ or $\lambda = 1$, we find results as shown in figure 10. It is seen that for small and large L the choice of λ is not very important, but for intermediate L the solutions are more sensitive to λ.

In figure 11 is shown what the effect is of choosing various values of ξ. Here we kept λ at the constant value of $\lambda = 0.75$. The influence of the choice of ξ seems almost negligible.

5 Conclusions

A theory is presented to calculate acoustic modes in a duct which is lined with porous material, divided into annular segments by rigid partitions. The partitions prohibit sound propagation between adjacent segments. The liner may be covered by a porous plate with given impedance.

It appears that single modes can not exist. Therefore, a method is developed to obtain *approximate* solutions of the eigenvalue problem. Results of this method seem trustworthy, especially for small pitch and for large pitch.

Numerical results suggest that the pitch length L seems only relevant for upstream modes of which the axial wave numbers have relatively small imaginary parts. It is observed that the eigenvalues for increasing L vary between the eigenvalues of the two limit cases, $L \to 0$ and $L \to \infty$. These limit eigenvalues are solutions of eigenvalue equations, found in the literature.

The new method, described in this paper, can be incorporated in an existing liner design procedure (Ref. 5). Moreover, it provides a tool to check the validity of the approximations for $L \to 0$ and $L \to \infty$.

6 References

1. Ingard, K.U., Locally and non-locally reacting flexible porous layers; a comparison of acoustical properties, *Transactions of the ASME* 103, 1981, pp. 302-313.
2. Morse, P.M., and Ingard, K.U., *Theoretical acoustics*, McGraw-Hill, New York, 1968.
3. Nayfeh, A.H., Kaiser, J.E., and Telionis, D.P., Acoustics of aircraft engine-duct systems, *AIAA Journal* 13 (2), 1975, pp. 130–153.
4. Sun, J., Effects of isotropic and anisotropic bulk liners on wave propagation in duct carrying flows, PhD thesis, Virginia Polytechnic Institute and State University, 1975.
5. Rienstra, S.W., The acoustics of a lined duct with flow, NLR Technical Report 87002, 1987.
6. Nilsson, B.E, *The Propagation of Sound in Cylindrical Ducts with Mean Flow and Bulk-reacting Lining*, Thesis University of Gothenburg, Sweden, 1980.
7. Cummings, A., Chang, I.-J., Sound attenuation of a finite length dissipative flow duct silencer with internal mean flow in the absorbent, *Journal of Sound and Vibration* 127 (1), 1988, pp. 1-17.
8. Bies, D.A., Hansen, C.H., Bridges, G.E., Sound attenuation in rectangular and circular cross-section ducts with flow and bulk-reacting liner, *Journal of Sound and Vibration* 146 (1), 1991, pp. 47-80.
9. Scott, R.A., The propagation of sound between walls of porous material, *Proceedings of the Physical Society* 58, 1946, pp. 358-368.
10. Bies, D.A., Acoustic properties of porous materials, in *Noise and vibration control*, edited by L.L. Beranek, McGraw-Hill, New York, 1971, pp. 245-269.
11. Rienstra, S.W., Contributions to the theory of sound propagation in ducts with bulk-reacting lining, *Journal of the Acoustical Society of America* 77 (5), 1984, pp. 1681-1685.
12. Eversman, W., Approximation for thin boundary layers in the sheared flow duct transmission problem, *Journal of the Acoustical Society of America*, Vol. 53, No. 5, 1973, pp. 1346-1350.

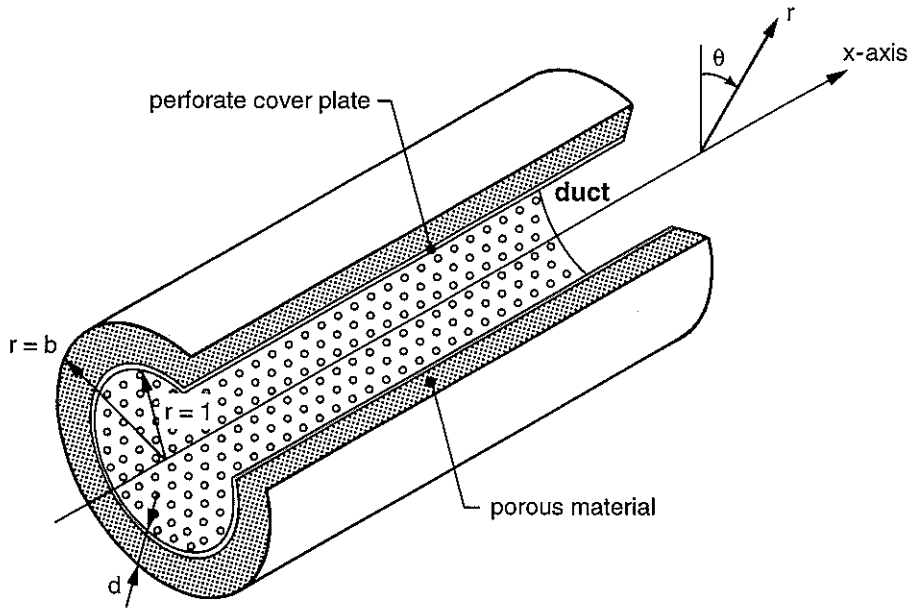

Fig. 1 Liner configuration

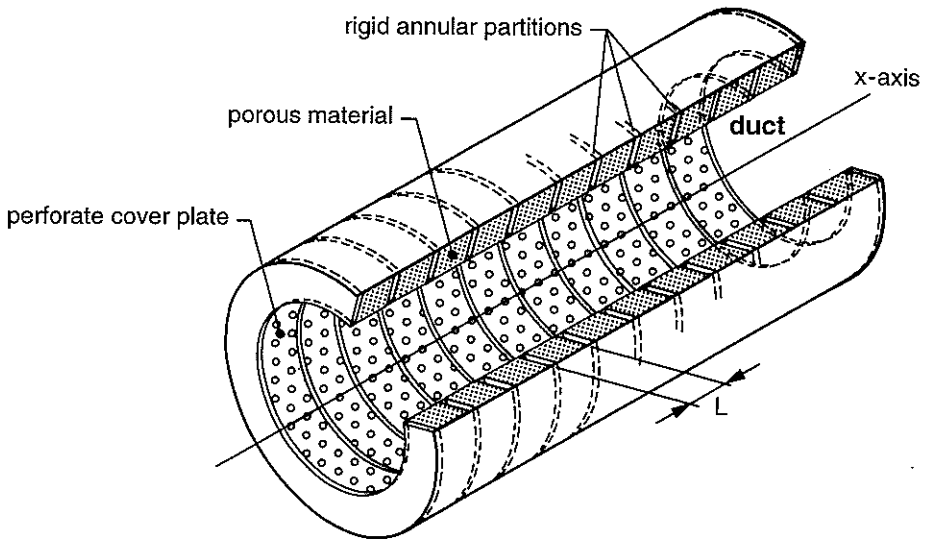

Fig. 2 Liner configuration with annular partitioning

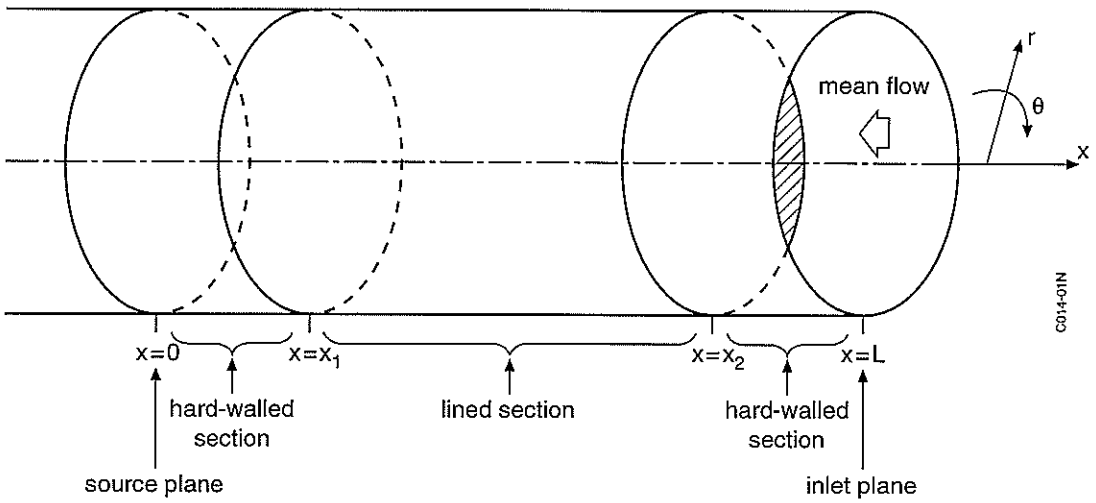

Fig. 3 Duct geometry

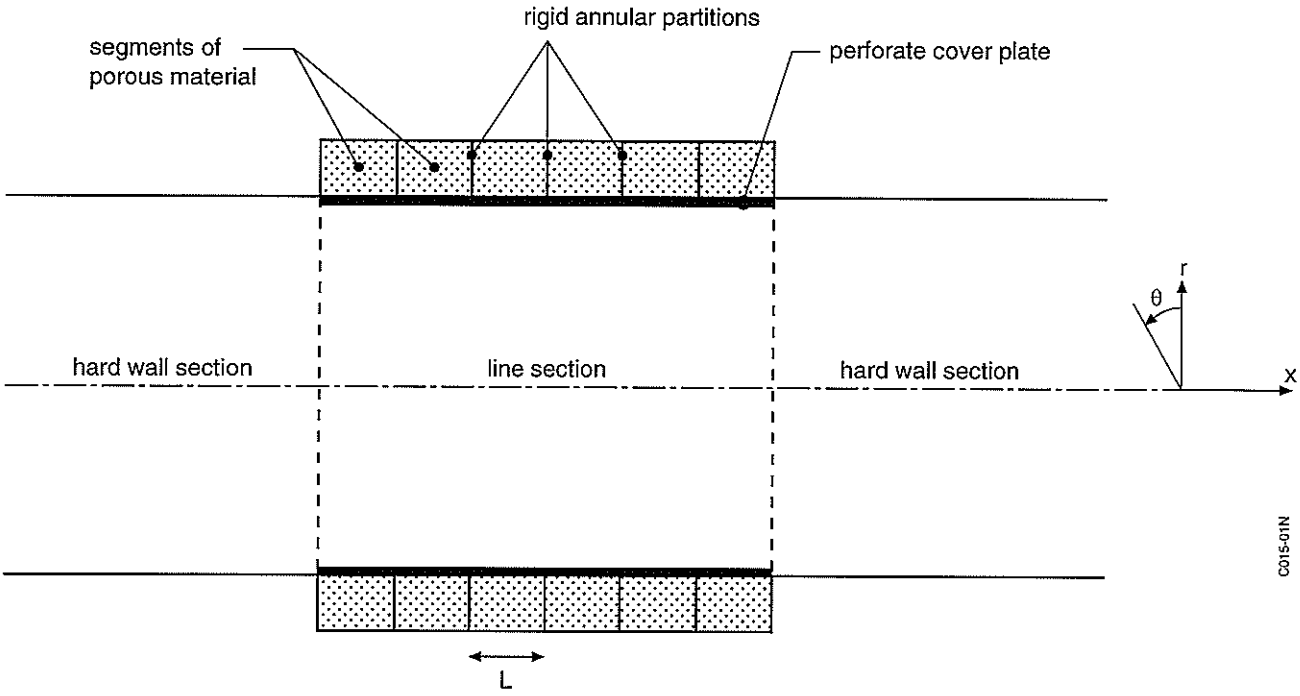

Fig. 4 Geometry of duct with bulk-absorbing liner

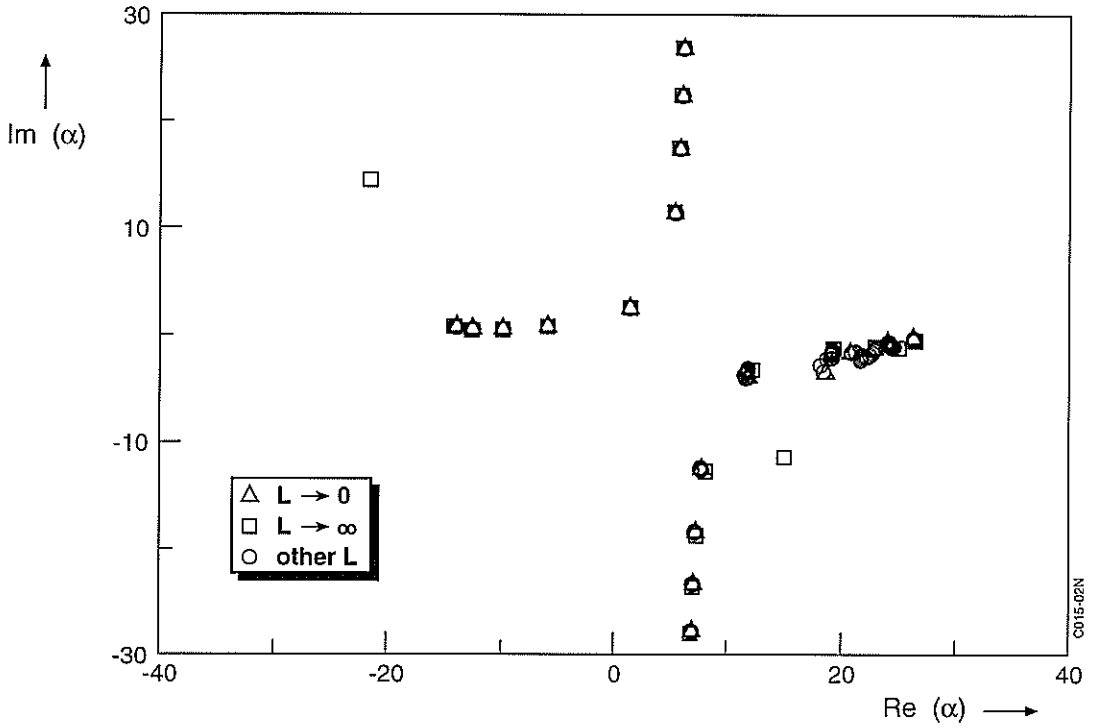

Fig. 5 Eigenvalues

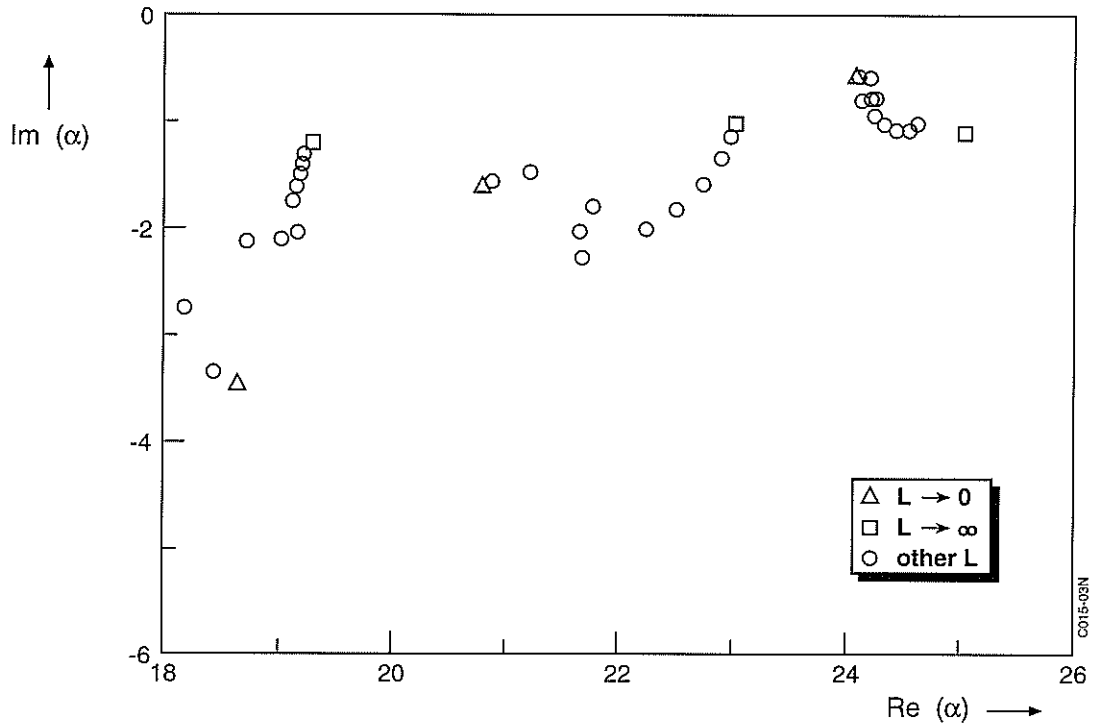

Fig. 6 Eigenvalues, enlarged view of figure 5

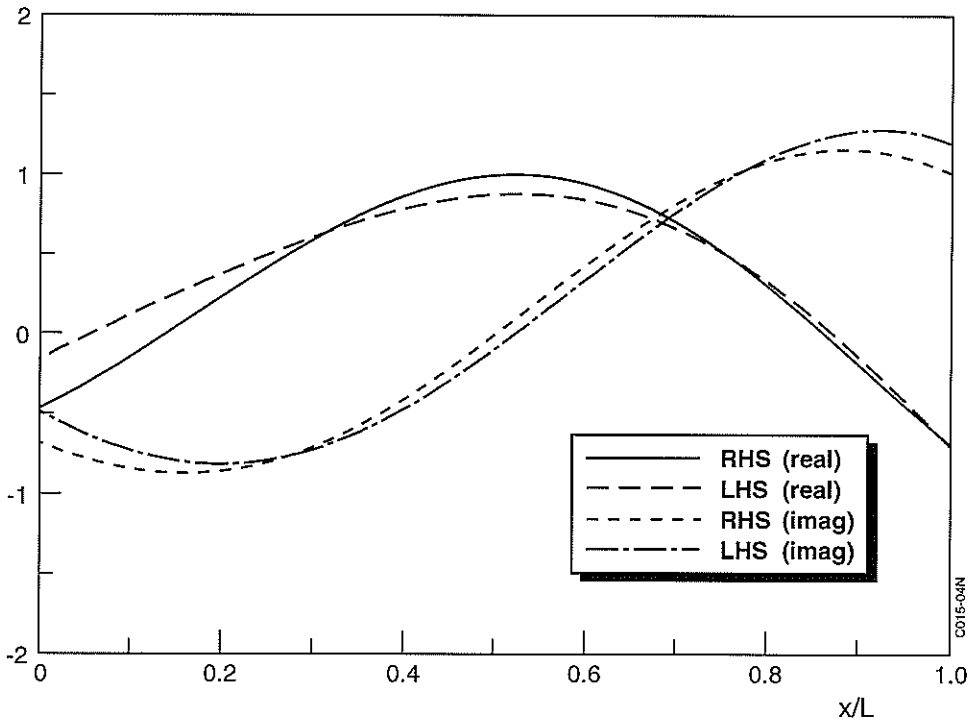

Fig. 7 Left hand side and right hand side of (16)

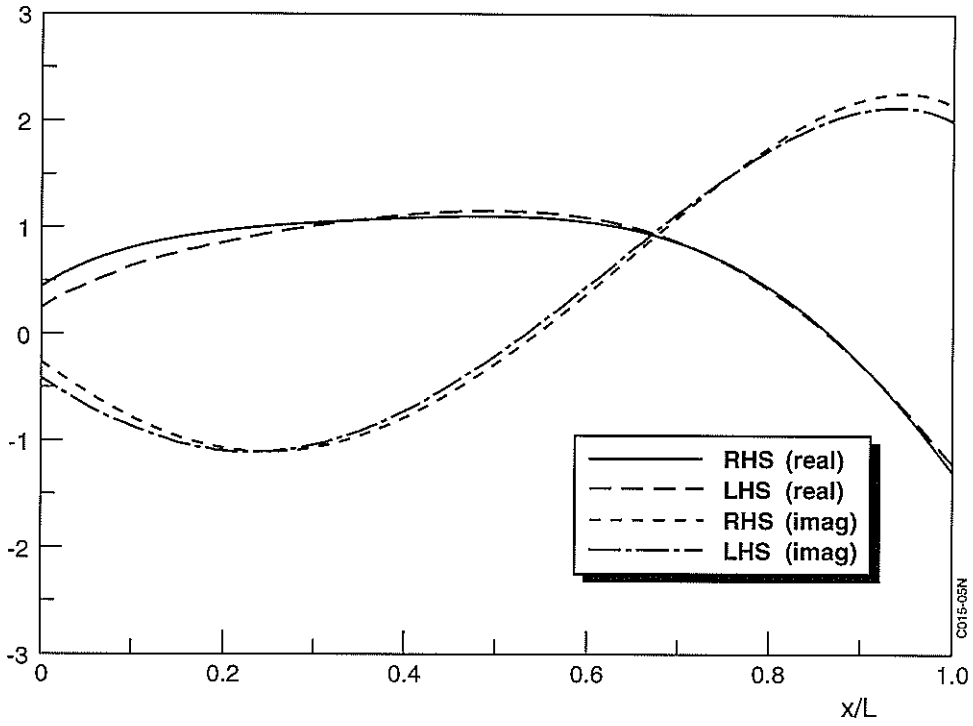

Fig. 8 Left hand side and right hand side of (17)

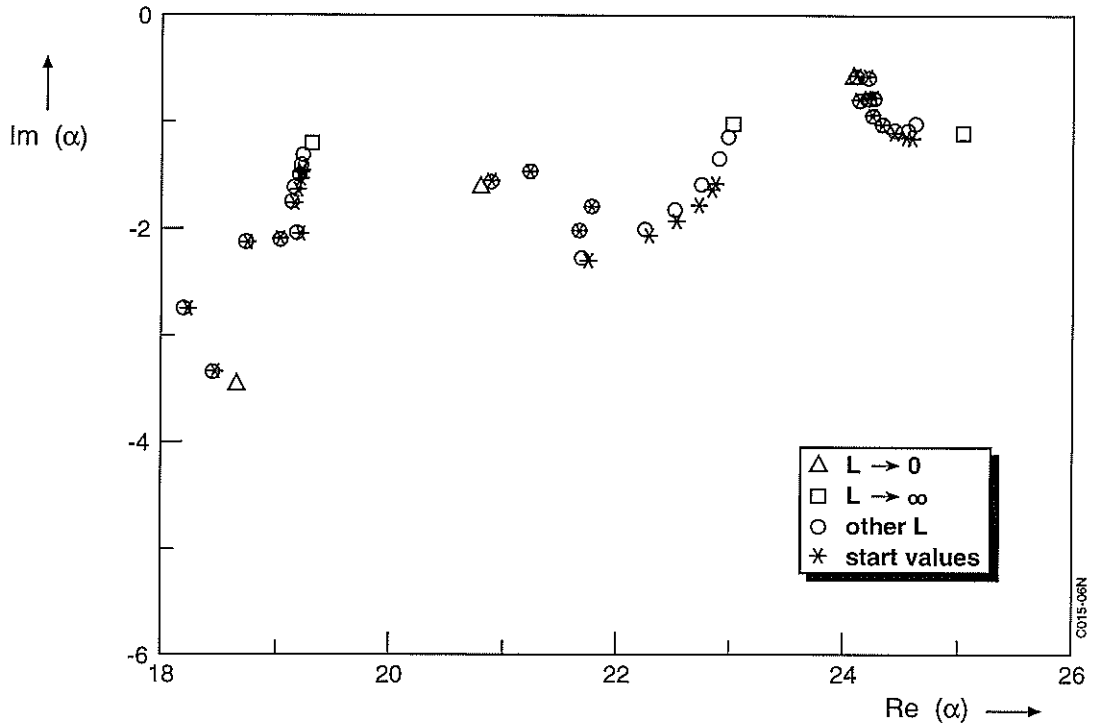

Fig. 9 Eigenvalues, comparison with solutions of (33)

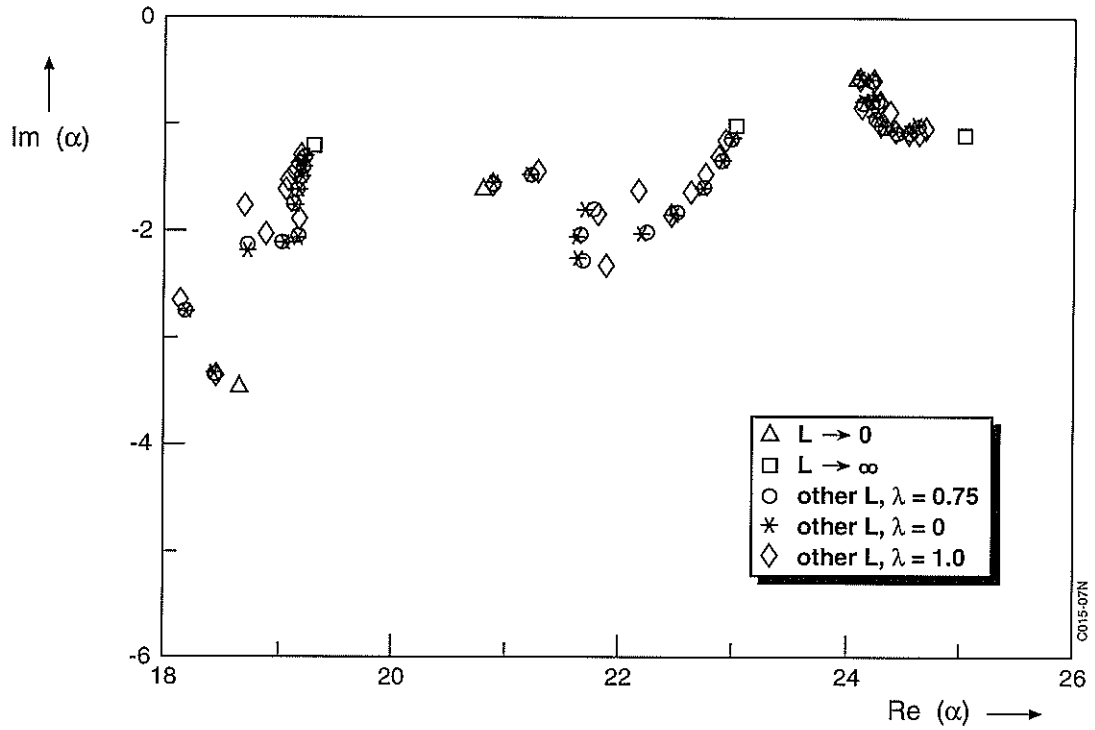

Fig. 10 Eigenvalues, influence of λ

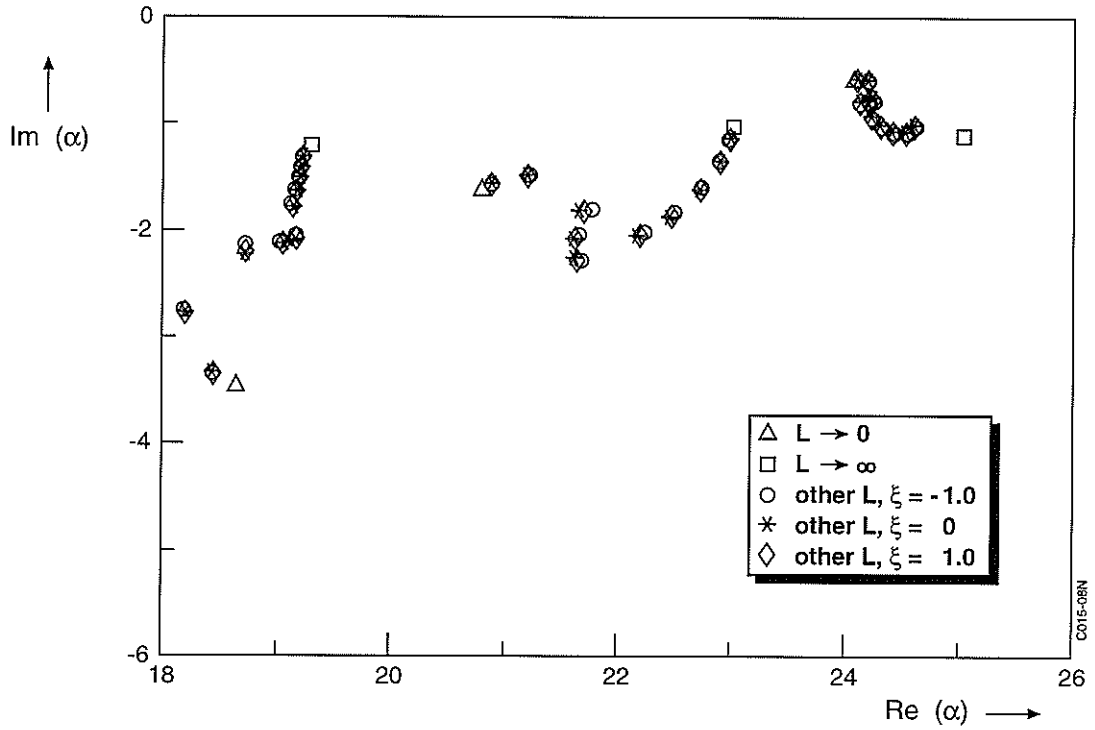

Fig. 11 Eigenvalues, influence of ξ

This page is intentionally left blank.

Appendix

A Limit cases

A.1 Infinitely large pitch

In case of an infinitely large pitch, there are no reflections at $x = x_1$ and $x = x_2$ and we can write instead of (8):

$$p^+(x,r,\theta) = f^+(r)\, e^{i(\alpha x + m\theta)}. \tag{A.1}$$

By applying (3) and the boundary condition at $r = b$, we obtain

$$p^+(x,r,\theta) = B \frac{J_m(\zeta r)Y_m'(\zeta b) - Y_m(\zeta r)J_m'(\zeta b)}{\zeta\left\{J_m'(\zeta)Y_m'(\zeta b) - Y_m'(\zeta)J_m'(\zeta b)\right\}} e^{i(\alpha x + m\theta)}, \tag{A.2}$$

with

$$\zeta^2 = \mu^2 - \alpha^2. \tag{A.3}$$

Then the boundary conditions are:

$$\frac{i\omega}{(\omega + M\alpha)^2} A = -\frac{1}{i\mu Z_c} B \tag{A.4}$$

and

$$\frac{(\omega + M\alpha)^2}{i\omega} F_m(\varepsilon) + i\mu Z_c G_m(\zeta, b) = Z_0. \tag{A.5}$$

Equation (A.5) is the "eigenvalue equation", from which the solutions α have to be solved. It is the same equation as in reference 9 (see also Ref. 11), although there $M = 0$.

A.2 Infinitesimally small pitch

When the pitch is very small, there is no axial sound propagation inside the liner. We can again start with expression (A.1), but, when applying the Helmholtz equation (3), we have to

omit the x-differentiations. The result is

$$p^{+}(x,r,\theta)=B\frac{J_m(\mu r)Y_m'(\mu b)-Y_m(\mu r)J_m'(\mu b)}{\mu\left\{J_m'(\mu)Y_m'(\mu b)-Y_m'(\mu)J_m'(\mu b)\right\}}e^{i(\alpha x+m\theta)}. \tag{A.6}$$

Then the eigenvalue equation becomes

$$\frac{(\omega+M\alpha)^2}{i\omega}F_m(\varepsilon)=Z_0-i\mu Z_c G_m(\mu,b). \tag{A.7}$$

This is the same result as in reference 11. The term with G_m is put into the right hand side, since it does not depend on the unknown eigenvalue α. The right hand side of (A.7) is, in fact, a given effective wall-impedance, dependent only on m.

A.3 Locally reacting liner

In a locally reacting liner there is only sound propagation in radial direction. Again, we can start with expression (A.1) and, when applying the Helmholtz equation (3), we have to omit the differentiations both in the x- and in the θ-direction. Then we have

$$p^{+}(x,r,\theta)=B\frac{J_0(\mu r)Y_0'(\mu b)-Y_0(\mu r)J_0'(\mu b)}{\mu\left\{J_0'(\mu)Y_0'(\mu b)-Y_0'(\mu)J_0'(\mu b)\right\}}e^{i(\alpha x+m\theta)} \tag{A.8}$$

and the eigenvalue equation becomes:

$$\frac{(\omega+M\alpha)^2}{i\omega}F_m(\varepsilon)=Z_0-i\mu Z_c G_0(\mu,b). \tag{A.9}$$

The right hand side of (A.9) is the impedance of a conventional liner in which the Helmholtz resonators are filled with porous material.

A good approximation for G_m is:

$$G_m(\gamma,b)\approx\frac{1}{(\gamma^2-m^2)^{1/2}\tan\left[d(\gamma^2-m^2)^{1/2}\right]}, \tag{A.10}$$

where $d = b-1$, i.e., the liner thickness. It implies for (A.9):

$$\frac{(\omega+M\alpha)^2}{i\omega}F_m(\varepsilon)\approx Z_0-\frac{iZ_c}{\tan(d\mu)}. \tag{A.11}$$

This is a more common expression for a locally reacting liner than (A.9). Note that air is modelled by $Z_c = 1$ and $\mu = \omega$.